Science of the Total Environment 957 (2024) 177677

Contents lists available at ScienceDirect

Science of the Total Environment

journal homepage: www.elsevier.com/locate/scitotenv

Site-dependent carbon and greenhouse gas balances of five fen and bog soils after rewetting and establishment of *Phalaris arundinacea* paludiculture

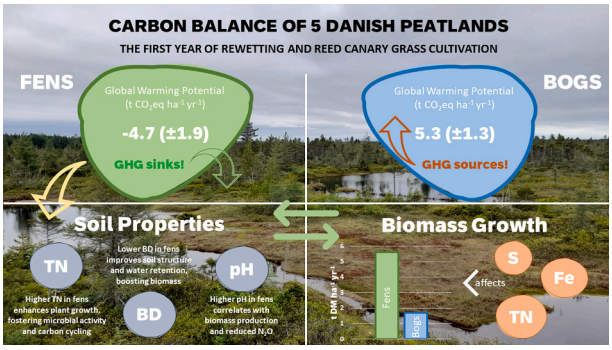
C.K. Nielsen [a,b,*], L. Elsgaard [a,c], P.E. Lærke [a,b]

[a] Department of Agroecology, Faculty of Technical Sciences, Aarhus University, Blichers Alle 20, 8830 Tjele, Denmark
[b] CBIO, Centre for Circular Bioeconomy, Aarhus University, Denmark
[c] iClimate, Interdisciplinary Centre for Climate Change, Aarhus University, Denmark

HIGHLIGHTS

- The highest GHG mitigation potential by paludiculture on fen peatlands
- All fens were sinks of C after rewetting and paludiculture (−1.3 to −11.5 t CO_2eq ha^{-1} yr^{-1}).
- Methane emissions were site-specific and depending on biomass growth, bulk density, and iron content in soil.

GRAPHICAL ABSTRACT



ARTICLE INFO

Editor: Jan Vymazal

Keywords:
Rewetting
Peatland
Carbon balance
Greenhouse gases
Paludiculture
Reed canary grass

ABSTRACT

Peatlands cover 3 % of the Danish land area, but drainage of these areas contributes to approximately 25 % of the total agricultural greenhouse gas (GHG) emissions. Paludiculture, defined as agriculture on wet or rewetted peatlands, has been proposed as a strategy to mitigate GHG emissions while keeping up production. However, little is known about the net GHG effects during establishment and how it is influenced by soil biogeochemical conditions. In this study, we determined annual carbon balances of five Danish peatlands, three fens and two bogs, for the first year of cultivation with reed canary grass (RCG) with two annual cuts in a mesocosm set-up under controlled conditions. Biomass yields were highly variable, ranging between 0.8 and 7.4 t dry matter (DM) ha^{-1} yr^{-1}, and significantly higher on fen peat soils. Ecosystem respiration (R_{eco}) fluxes of CO_2 were naturally highest from sites with high biomass establishment. Methane emissions were site-specific, ranging between 0.03 and 1.85 t CH_4 (CO_2eq ha^{-1} yr^{-1}), and affected by biomass growth, as well as bulk density and the iron content within soil. Nitrous oxide fluxes were negligible, despite nitrogen (N) fertilisation with 200 kg N ha^{-1} yr^{-1}. Driven by net primary production (NPP) we found that the fen sites were GHG sinks, with a global warming potential (GWP) of −1.3 to −11.5 t CO_2eq ha^{-1} yr^{-1} during the first year of rewetting and RCG establishment. The bogs remained sources of carbon (5.3 t CO_2eq ha^{-1} yr^{-1}). Our results highlighted that the

* Corresponding author at: Department of Agroecology, Faculty of Technical Sciences, Aarhus University, Blichers Alle 20, 8830 Tjele, Denmark.
E-mail address: claudia@agro.au.dk (C.K. Nielsen).

https://doi.org/10.1016/j.scitotenv.2024.177677
Received 4 June 2024; Received in revised form 21 October 2024; Accepted 18 November 2024
Available online 29 November 2024
0048-9697/© 2024 The Authors. Published by Elsevier B.V. This is an open access article under the CC BY license (http://creativecommons.org/licenses/by/4.0/).

nutrient-rich Danish fen peatlands showed a potential for GHG mitigation by paludiculture under extensive agricultural management, while this was not the case for the bog sites due to poor biomass establishment. In conclusion, we found the highest GHG mitigation potential by rewetting and RCG paludiculture on nutrient-rich fen peatlands.

1. Introduction

Climate change is one of the greatest threads in our times (Solomon et al., 2009) and its adverse effects are occurring at a rapid pace. In order to mitigate extreme global warming and the associated consequences, the goal to reach net-zero greenhouse gas emissions (GHG) is on the agenda in all governmental and private sectors (Liobikienė and Butkus, 2017). However, with a substantial contribution of approximately >350 Pg carbon dioxide equivalents (CO_2eq) to the global net emissions, the soil-atmosphere exchange of GHGs plays a critical part in affecting global climate change (Oertel et al., 2016; Smith et al., 2018). In particular crop cultivation on drained organic soils is known to play a substantial role in the GHG budget, annually emitting approximately 830 million t CO_2eq (Conchedda and Tubiello, 2020). Naturally, peatlands are characterised by an organic carbon (C) content of >12 % due to the accumulation and preservation of dead plant debris under anaerobic conditions (Montanarella et al., 2006). As one tool in the toolbox of GHG mitigation strategies, the re-establishment of these natural C sinks has become a fundamental point on the agenda of various global, national, and regional climate actions. However, since drained peatlands play a role in agricultural economics (Chapman et al., 2003; Juutinen et al., 2020), questions remain regarding potentially profitable land-use options that can meet the goal of GHG reduction. Paludiculture, defined as biomass production on wet or rewetted peatlands, is one agricultural alternative and has been proposed as an incentive to accelerate peatland rewetting (Tanneberger et al., 2020) due to the provision of economic revenues from biomass production while potentially reducing carbon dioxide (CO_2) emissions from soil respiration (Lahtinen et al., 2022). However, while the green transition and a change in lifestyle poses potential marked opportunities for paludiculture biomass: e.g., for bioenergy (Jensen and Eller, 2020; Hartung et al., 2020), alternative building materials (Ziegler et al., 2021), or as a substitute for soy protein (Nielsen et al., 2021a), no clear consensus on the GHG reduction efficiency by paludiculture has been reached yet.

One factor is the variety of perennial plants chosen for cultivation as a paludicrop. Biomass is the key component in an ecosystems carbon balance: driving the difference between gross primary production (GPP) and thus photosynthetic uptake of CO_2 and subsequent loss of CO_2 to the atmosphere by ecosystem respiration (R_{eco}). In this context, the plant species and its yield under cultivation will affect net C balances. One suitable perennial plant for cultivation in paludiculture is reed canary grass (*Phalaris arundinacea)* (RCG), where high yields have been reported from wet peat soils (Karki et al., 2019). However, not only biomass performance (McCarthy and Enquist, 2007), but also magnitudes of associated GHG exchange dynamics from plant and soil, are highly depending on site-specific differences in environmental factors (Juszczak et al., 2013). In particular water table depth (WTD) (Evans et al., 2021), microclimate and -topography (Asemaninejad et al., 2019) and precipitation patterns (Huth et al., 2018), but also differences in soil biogeochemical properties are crucial variables, significantly affecting the site-specific magnitudes of GHG dynamics (Nielsen et al., 2023). In addition, there is limited knowledge regarding GHG dynamics during the establishment phase of paludiculture. This applies to both, net ecosystem exchange (NEE) and, in particular, methane (CH_4) dynamics, which are known to show temporal patterns during the transition towards a fully-rewetted state (Kalhori et al., 2024).

In a Danish context, we are aware of sixteen studies regarding GHG emissions of either CO_2, CH_4 or nitrous oxide (N_2O) of cultivated peatlands. Of these, only three in-situ studies (Karki et al., 2019; Kandel et al., 2019; Kandel et al., 2020), and three mesocosm experiments (Karki et al., 2014; Karki et al., 2015; Karki et al., 2016) determined atmospheric GHG exchange from peatland rewetting and RCG paludiculture. However, these studies were all performed on one single fen peatland site. With current ambitions of rewetting 30 % of the Danish agricultural soils (Ministry of Food, Agriculture and Fisheries of Denmark, 2021), there is the need to comparably document magnitudes and variation of the GHG mitigation potentials for different peatland sites during rewetting and the establishment of RCG. In this context, mesocosm experiments have shown to be a sound technique (Stewart et al., 2013) to assess soil-specific drivers and magnitudes for carbon balances.

Thus, we hypothesised that there will be considerable variation of GHG dynamics and site-specific C sink potentials for Danish peatland sites following rewetting and cultivation with RCG. The aims of this study were to: 1) determine the variation in net C balances for different Danish peatlands during rewetting and cultivation of RCG, and 2) assess the mitigation potential of RCG paludiculture with regards to the global warming potential (GWP).

2. Methods

2.1. Experimental design and set-up

The study was performed in a controlled semi-field set up from 21st of June 2019 to the 20th of June 2020 at Aarhus University Viborg, Denmark (56°48′54N, 9°58′30″E). The region is part of the Atlantic mire zone and has a temperate climate characterised by windy winters and cool summers. The annual average air temperature was 9.2 °C and the annual precipitation was 936 mm during the study period (Fig. A1). Monthly average soil temperature in 10 cm depth ranged between 3.5 °C (Dec. 2019) – 17.7 °C (July 2019). For the study, 5 intact soil mesocosms (30 cm diameter x 60 cm height) were collected in March 2019 from each of the five Danish peatlands - the bogs (B): Lille Vildmose (B_{LV}), and Store Vildmose (B_{SV}); as well as the fens (F): Øby ($F_Ø$), Selkær Enge (F_{SE}), and Vejrumbro (F_V) (Table 1).

All sites were shallow-drained at the time of sample collection and are classified as permanent grassland. The peatland sites used for this study, including their land-use history, have been in detail described in Nielsen et al. (2023). Sampling resulted in a total of 25 mesocosms, which were placed in containers for water table depth (WTD) control within a ditch (1 m deep x 1 m wide x 8 m long) at the semi-field facilities. A detailed description of the procedure of mesocosm collection, as well as details on the build-up of containers including WTD adjustment and stabilisation can be found in Nielsen et al. (2023) as well as in the supplementary material (Fig. A5). For each mesocosm, original vegetation, was removed and the WTD was constantly held at −5 cm below soil surface. Vegetation removal resulted some removal of the upper 5 cm of topsoil. The mesocosms were continuously, but equally, exposed to fluctuations in natural environmental conditions (e.g., wind, temperature, radiation, and precipitation). Reed canary grass (RCG) (*Phalaris arundinacea*, cultivar: Lipaula) was sown by hand at a seeding rate of 25 kg ha^{-1} in April 2019. After emergence of the seeds, the mesocosm received fertilisation with 40 kg N ha^{-1}, 9 kg P ha^{-1}, and 43 kg K ha^{-1}, using 286 kg ha^{-1} of combined NPK fertiliser with a grade of 14–3-15. Prior to the start of GHG measurements, on the 17th of June 2019, biomass was trimmed to stubble height. RCG biomass was harvested twice: on the 27th of September 2019 and the 19th of June 2020. On the 24th of June 2019 and the 20th of April 2020, the cultivated

mesocosms received split-fertiliser applications with a total of 200 kg N ha^{-1} yr^{-1} and 200 kg K ha^{-1} yr^{-1} in equal doses (Fig. A2). Biomass development was continuously monitored by height measurements on each of the gas sampling campaigns. On each of the harvest occurrences, grass was manually cut at stubble height and immediately brought to the laboratory for determination of fresh weight and subsequently dry-matter (DM) by oven-drying at 60 °C until constant weight.

2.2. Environmental variables, control of soil water saturation, and soil properties

Hourly values for air temperature and precipitation over the entire study period were collected from the meteorological station at Aarhus University Viborg, approximately 1 km away from the semi-field facilities. Five soil mesocosms, one for each peatland site, were equipped with a piezometer for control of WTD stability, time domain reflectometry (TDR) probes, and a soil temperature probe at −10 cm depth, logging temperature automatically every hour. WTD monitoring of the mesocosms was performed during GHG sampling campaigns, as well as during extreme wet or warm periods. Further, dielectric permittivity (ε) and the volumetric water content (θ) were measured during sampling campaigns using the TDR probes. However, values were not calibrated for the various sites and therefore only show differences between sites, not actual values of θ. Data on the following soil physical and chemical properties for the various sites over a depth of 60 cm were gathered from Nielsen et al. (2023): total nitrogen (TN), total carbon (TC), total iron (Fe), potassium (K), phosphorus (P) and sulfur (S), bulk density (BD) and pH.

2.3. Flux measurements of CO_2, CH_4, and N_2O

Flux measurements of CO_2, CH_4, and N_2O were performed in biweekly intervals between 9:30 and 14:30, resulting in a total of 27 measurement campaigns. Gas fluxes were measured from the non-instrumented mesocosms using the opaque chamber method and round (30 cm diameter x 50 cm height, 41.9 L) polyvinyl chloride (PVC) chambers, equipped with fans and vents, as well as a temperature probe. The sampling order on each campaign was randomised and five gas samples were withdrawn via a 1.2 m polypropylene tube of 4 mm inner diameter using a syringe (20 mL) at 0, 5, 10, 25, and 50 min after chamber closure. 16 mL of dead air within the tube-system was removed with a syringe and discarded. Subsequently, 11 mL of mixed air from the chamber was transferred to evacuated glass exetainers (6 mL; Labco Limited, UK). The filled exetainers were stored dark until analysis within 30 days on a gas chromatograph (GC; Agilent 7890, Agilent A/S, Nærum, Denmark), equipped with an automatic injection system (CTC CombiPAL, Agilent A/S, Nærum, Denmark). Details on the GC instrument calibration were in detail described by Petersen et al. (2012).

2.4. Flux calculation

Gas fluxes were calculated with the *flux* package (Jurasinski et al. (2014) version 0.3–0) in R (R core team (2021) version 4.1.4 "Bird Hippie"), using linear regression based on best fits according to smallest normalised root mean square errors (NRMSE). Fluxes were calculated from at least four out of the five gas concentration measurements. Additional quality checks for the individual fluxes include R^2, the number of measurements below ambient concentrations (NOMBA) and a GC quality flag to indicate observed errors resulting from the GC analysis. In addition, we controlled concentrations of CH_4 and N_2O for potential chamber or vial leakage by testing against CO_2 concentration data. Details on the various quality flags are in detail described in the *flux* package documentation (Jurasinski et al., 2014). We accepted fluxes of CO_2 when: 1) quality flags were not breached, 2) $R^2 > 0.95$, and 3) $p < 0.05$. Fluxes of CH_4 and N_2O were accepted when: 1) quality flags were not violated, and 2) $R^2 > 0.90$. In order to avoid over- or under-estimation, a total of $n = 26$ gas fluxes beyond the 2.0 percentile tail of a log-norm-distribution were discarded as outliers. No CH_4 fluxes below -0.5 mg m^{-2} h^{-1} were found, and no fluxes were discarded due to leakage. Hence, out of initially 540 fluxes for each gas, 87 %, 84 % and 77 % of measured CO_2, CH_4, and N_2O fluxes, conformed to quality requirements.

2.5. Interpolation to annual values

2.5.1. CO_2

Hourly CO_2 fluxes from ecosystem respiration (R_{eco}), for each of the mesocosms were modelled using the Lloyd and Taylor (1994) modified Arrhenius-type equation (Eq. (1)), for periods in between biomass harvest occurrences, and based on best fits with hourly soil temperature data:

$$R_{eco} = \theta_{10} * exp\left(E_0 * \left(\frac{1}{T_{ref} - T_0} - \frac{1}{Temp - T_0}\right)\right) \quad (1)$$

Eq. (1): Where R_{eco} is the ecosystem respiration flux rate; θ_{10} is the base respiration rate (μmol C m^{-2} s^{-1}); T_{ref} is the reference temperature (10 °C); E_0 is the parameter of R temperature sensitivity; T_0 is the theoretical lower temperature limit for soil respiration (−46.02 °C); and Temp is the soil temperature (°C) at − 10 cm.

Subsequently, hourly values were summed up to annual cumulative CO_2 emissions. An interpolation error was estimated using the Monte-Carlo jackknife method, run with 100 iterations (Beetz et al., 2013).

2.5.2. CH_4 and N_2O

Hourly values of CH_4 for 1) each of the mesocosms, and 2) each peatland site, were calculated by a simple linear regression model (Eq. (2)) and under consideration of daily soil temperatures as for CO_2:

Table 1
Agricultural peatland sites, their peatland type and geographic location for mesocosm excavation in this study. Site-averaged soil properties of 60 cm depth for total carbon (TC), total nitrogen (TN), bulk density (BD), pH, and the minerals iron (Fe), potassium (K), phosphorus (P) and sulfur (S). Values for Fe, K, P, and S are given in g kg^{-1} dry matter. All soil properties were previously reported by Nielsen et al. (2023). Letters indicate differences between means, where treatments with the same letter are not significantly different.

Site	Location	Type	TC %	TN %	BD	pH	Fe	K	P	S
Lille Vildmose (B_{LV})	56°55"N, 10°12′28″E	Oligotrophic raised bog	46.79 ab	1.43 b	0.11 b	4.6 c	1.48 c	0.49 a	0.57 b	2.92 c
Store Vildmose (B_{SV})	57°11′25"N, 9°49′4″E	Highly degraded oligotrophic raised bog	51.27 a	1.32 b	0.08 b	5.2 b	1.04 c	0.83 a	0.52 b	3.21 c
Øby ($F_{Ø}$)	56°27′28"N, 9°40′32″E	Minerotrophic riparian fen	41.27 bc	2.85 a	0.17 a	6.2 a	8.04 b	0.51 a	1.29 a	11.47 a
Selkær Enge (F_{SE})	56°27′47"N, 10°44′38″E	Highly degraded minerotrophic fen	36.58 c	2.73 a	0.19 a	6.4 a	10.74 a	0.78 a	1.14 a	9.83 ab
Vejrumbro (F_V)	56°26′11"N, 9°33"E	Minerotrophic riparian fen	35.15 c	2.63 a	0.21 a	5.3 b	8.38 b	0.93 a	1.18 a	7.13 b

$$R_{CH_4} = \theta_1 * \theta_2 * Temp \quad (2)$$

Eq. (2): R_{CH4} = CH_4 flux rate, θ_1 = base respiration rate (in μmol C m^{-2} s^{-1}) at the reference temperature (T_{ref}) of 10 °C, θ_2 = bias coefficient, Temp = soil temperature (°C).

Annual emissions of N_2O were determined following the trapezoidal rule in combination with a Monte Carlo permutation (Huth et al., 2013). For both gases, values were summed up to annual balances, followed by the application of bootstrap and jackknife methods to determine the interpolation error for integration. The applied jackknife and bootstrap methods have been in detail described by Köhler et al. (2012) and Nielsen et al. (2023).

2.5.3. Global warming potential

To determine the 100-yr global warming potential (GWP), annual cumulative fluxes of CH_4 and N_2O were converted into CO_2 equivalents (CO_2eq) using conversion factors of 28 for methane and 265 for nitrous oxide (Myhre et al., 2013), as adopted by the UN Framework Convention on Climate Change (UNFCCC) in 2021.

2.6. Carbon balances

We calculated autotrophic respiration (R_a) based on measured and modelled fluxes for R_{eco} and heterotrophic respiration (R_h). The latter was previously defined for the same peatland sites at equal WTD in the same experimental period (Nielsen et al., 2023). Annual biomass yield was calculated based on DM yields for each of the harvests. Balances of net primary productivity (NPP), gross primary production (GPP), and net ecosystem exchange (NEE) for each mesocosm were calculated following the revised root:shoot ratio (R/S) assessment for paludiculture plants under different harvest frequencies as described in detail by Nielsen et al. (2021b). For the estimation of NPP, we used the R/S of 1.2 for RCG with two annual cuts, and a TC content of 45.4 % for aboveground and stubble biomass, and 43.5 % for belowground biomass. The net ecosystem carbon balance (NECB) was determined based on NEE and the export of C by biomass harvest (Elsgaard et al., 2012; Eickenscheidt et al., 2015). We used the atmospheric sign convention for C exchange, where negative values represent uptake, and positive values losses to the atmosphere. All carbon balances were calculated in t C ha^{-1} yr^{-1} for each of the mesocosms, followed by determination of means and standard error for the different soil types. The final GWP was corrected for export of C by biomass harvest, according to Beetz et al. (2013) and Eickenscheidt et al. (2015) and expressed in t CO_2-C eq ha^{-1} yr^{-1} as well as t CO_2eq ha^{-1} yr^{-1}. Details on the equations used for the calculations of carbon balances are presented in Table B1.

2.7. Statistical analysis

For all co-variates, as well as GHG fluxes and measurements, observations are given as means, and standard errors ($n = 4$) are reported to present the distribution of data around means. To test for significant differences between means, we performed one-way ANOVA with post-hoc Tukey's HSD tests at 95 % confidence levels. Correlation effects between site-specific biomass yields and soil properties were assessed by multiple linear regression using Pearson's correlation.

We used generalised additive models (GAMs) to assess the effects of predictor variables on 1) gas fluxes of CO_2 and CH_4 for individual sampling campaigns, 2) annual cumulative values for NEE and CH_4-C, as well as 3) annual biomass yield and the GWP. This method has been chosen as a flexible approach considering both: linear and non-linear relationships, accounting for variable-specific data-derived penalties (Marra and Wood, 2011; Wood, 2011; Wood et al., 2016).

Response variables were log-transformed if necessary and GAMs were performed, using a gaussian distribution and identity link function, in the package *mgcv* (Wood, Version 1.8–39, 2022) in R (R Core Team (2021) Version 4.1.2 – "Bird Hippie"), using restricted marginal likelihood for all model coefficient and penalties. Before model fitting, we tested the variables in question for multicollinearity under consideration of the Pearson product moment correlation coefficient.

For gas fluxes of CO_2 and CH_4, we used the model in Eq. (3), while the model in Eq. (4) was used as the final model for annual cumulative values of NEE, CH_4-C, biomass yield, and the GWP:

$$\begin{aligned} &y_i \sim N\left(\mu, \sigma^2\right) \\ &y_i = \alpha + f_1(t.air_i, t.soil_i) + f_2 intrannual(date_i) + f_3(tdr_i) + f_4(S_i) \\ &+ f_5(Fe_i) + f_6(P_i) + f_7(pH_i) + f_8(BD_i) + f_9(TC_i) + f_{10}(TN_i) \\ &+ f_{11}(K_i) + f_{12}(Biomass_i) + \beta_1 x_1 + \varepsilon_i, \varepsilon_i \sim N(\mu, \sigma^2) \end{aligned} \quad (3)$$

$$\begin{aligned} &y_i \sim N\left(\mu, \sigma^2\right) \\ &y_i = \alpha + f_4(S_i) + f_5(Fe_i) + f_6(P_i) + f_7(pH_i) + f_8(BD_i) + f_9(TC_i) \\ &+ f_{10}(TN_i) + f_{11}(K_i) + f_{12}(Biomass_i) + \beta_1 x_1 + \varepsilon_i, \varepsilon_i \sim N(\mu, \sigma^2) \end{aligned} \quad (4)$$

Eqs. (3) and (4):Where y_i is the non- or log transformed observed dependent variable; μ is the overall mean, affected by f_1, the isotropic product smooth, representing marginal effects and interaction of air and soil temperature (t.air and t.soil); $f_2$intrannual(date) is the penalised cyclical smooth term of data; $f_3 - f_{12}$ are the smooth functions of various covariates for the ith sample; x_1 is the peatland type as a categorical variable (bog or fen); α is the intercept; and σ^2denotes the experimental error.

All model residuals were inspected for normality and homoscedasticity. All results from the four replicates per site are reported as mean ± standard error (SE), unless otherwise specified.

3. Results

3.1. Biomass yield and soil properties

Biomass growth per site was similar from the onset of the experiment until the first cut in September 2019, and after the first harvest until the second cut and end of experiment in June 2020 (Table 2). Harvested annual cumulative biomass yield was on average significantly ($p < 0.001$) higher from fen peatlands (5.6 ± 0.6 t DM ha^{-1} yr^{-1}) than from bog peatlands (1.7 ± 0.4 t DM ha^{-1} yr^{-1}), with the highest total yield found for F_{SE} (7.4 ± 1.3 t DM ha^{-1} yr^{-1}), and the lowest for B_{SV} (0.8 ± 0.2 t DM ha^{-1} yr^{-1}).

The Pearson's correlation detected significant ($p < 0.001$, $R = 0.79$) positive correlations between total annual biomass yields and soil contents of S (Figs. A3 and A4), as well as Fe, BD and TN ($R \geq 0.72$, $p < 0.01$). Contents of TC and the C/N ratio were negatively correlated ($p < 0.01$, R = -0.77). pH was positively ($p < 0.001$; $R > 0.8$) correlated to contents of S, P and Fe.

Table 2
Average harvested biomass yield (t DM ha^{-1} yr^{-1}) for the sites Lille Vildmose (B_{LV}), Øby ($F_Ø$), Selkær Enge (F_{SE}), Store Vildmose (B_{SV}) and Vejrumbro (F_V) and peatland types per harvest occurrence and as an annual total. Letters indicate differences between means, where treatments with the same letter are not significantly different.

Site	27th Sept 2019	20th June 2020	Total yield
B_{LV}	0.9 (± 0.2)bc	1.6 (± 0.3)bc	2.5 (± 0.4)bc
B_{SV}	0.3 (± 0.1)c	0.5 (± 0.2)c	0.8 (± 0.2)c
$F_Ø$	1.5 (± 0.3)ab	2.7 (± 0.6)ab	4.2 (± 0.9)ab
F_{SE}	2.8 (± 0.5)a	4.6 (± 0.8)a	7.4 (± 1.3)a
F_V	1.9 (± 0.1)ab	3.4 (± 0.2)ab	5.2 (± 0.3)ab
Bog	0.6 (± 0.1)b	1.1 (± 0.3)b	1.7 (± 0.4)b
Fen	2.1 (± 0.2)a	3.6 (± 0.4)a	5.6 (± 0.6)a

3.2. Measured fluxes of CO_2, CH_4, and N_2O

Annual average fluxes of CO_2 from R_{eco} ranged between 203 ± 23 mg m^{-2} h^{-1} (B_{SV}) to 463 ± 68 mg m^{-2} h^{-1} (F_V) (Table A1) and were highly affected ($p < 0.001$) by biomass growth (Fig. B1), with the highest fluxes from sites with most biomass growth. This was also depicted by CO_2 fluxes from fen peatlands being on average higher than flux magnitudes from bogs. For soil mesocosms with similar biomass growth (B_{LV} and $F_Ø$), average flux magnitudes were near equal (Fig. 1a). Measured fluxes of CH_4 were rather low for mesocosms with a WTD of −5 cm, ranging between 0.02 ± 0.01 mg m^{-2} h^{-1} (B_{LV}) to 0.92 ± 0.32 mg m^{-2} h^{-1} (B_{SV}) (Table A2). The high average CH_4 flux magnitude for soil from B_{SV} was due to three captured methane spikes >3 mg m^{-2} h^{-1}, though occurring simultaneously with high methane fluxes of lesser magnitudes from other peatland sites (Fig. 1b). For all soils, but in particular B_{LV}, we observed occasions of methane uptake, also during summer months. However, methane fluxes were highest with peaking biomass growth before harvest.

For both, magnitudes of CO_2 and CH_4 emissions, the GAM detected significant ($p < 0.001$) dependencies on biomass growth, measured by biomass height in cm (Table B2). Further, the interaction of soil and air temperatures affected ($p < 0.001$) flux magnitudes most of all parametric and smooth coefficients that were included in the GAM. However, CO_2 was rather affected by air than soil temperature (Fig. B2) as compared to CH_4, that showed a higher sensitivity to soil temperature (Fig. B4). The higher dependency on air temperatures for CO_2 is also reflected by the influence of date on flux magnitudes ($p < 0.001$), which were not found for CH_4. Further, peatland type had an effect ($p < 0.001$) on fluxes of CO_2. Among the biogeochemical soil properties, pH affected CO_2 flux magnitudes, while the content of Fe as well as BD significantly ($p < 0.001$) explained the variation in CH_4 fluxes (Fig. B3). Overall, the GAM allowed us to detect combined linear and non-linear trends with 85 % of the deviance explained for fluxes of CO_2, and 56 % for CH_4.

Nitrous oxide emissions were near zero (Fig. 1c), despite fertilisation, and negligible. Hence, emissions of N_2O were not included in further statistical analyses.

3.3. Annual cumulative emissions and carbon balances

Modelled hourly rates of R_{eco} showed a high seasonal variability depending on temperatures and biomass growth ($p < 0.001$), also when separated into components of R_h and R_a (Fig. 2). The export of carbon by biomass harvest was highest on F_{SE} (3.4 ± 0.6 t C ha^{-1} yr^{-1}) and lowest on soil mesocosms from B_{SV} (0.4 ± 0.1 t C ha^{-1} yr^{-1}) (Table 3). With R_h being similar for all soil sites, all calculated carbon balances were affected by NPP and the resulting harvested biomass yields. The calculated GPP ranged between −3.0 ± 0.5 (B_{SV}) to −12.9 ± 2.1 (F_{SE}) t C ha^{-1} yr^{-1}, resulting in a negative NEE (−2.5 ± 1.0 to −6.5 ± 1.6 t C ha^{-1} yr^{-1}) for those sites with strong biomass growth (F_{SE}, F_V, $F_Ø$) and near zero or positive (−0.4 ± 0.5 to 1.3 ± 0.3 t C ha^{-1} yr^{-1}) on sites where biomass was not successfully established (B_{LV} and B_{SV}, Fig. 3). With a deviance of 97 % explained, the GAM for budgets of annual NEE (t CO_2-C ha^{-1} yr^{-1}) determined not only biomass yields and peatland types as affecting ($p < 0.001$) annual NEE, but also found that soil fertility proxies of TN, TC and K were equally ($p < 0.001$) critical (Table B3).

However, while we found differences for carbon balances between peatland types, such differences were not found for annual cumulative emissions of CH_4. With a wide range between 0.03 ± 0.02 (B_{LV}) to 1.85 ± 0.67 (B_{SV}) CO_2eq t ha^{-1} yr^{-1}, the deviance for annual cumulative emissions of CH_4 was only to a lesser extend (57 %) explained by the GAM, where only peatland type ($p < 0.001$) and differences in site-specific BD ($p < 0.01$) illuminated part of the variation. The differences between the two peatland types were significant for all components of the calculated carbon balances.

Taking the export of C by biomass harvest into consideration and including dynamics of CH_4 and N_2O, we calculated GWPs ranging between −3.1 ± 0.9 (F_{SE}) to 2.2 ± 0.4 (B_{SV}) t CO2-C eq ha^{-1} yr^{-1}. There was a significant ($p < 0.001$) difference between 1) fen (−1.3 ± 0.5 t CO2-C eq ha^{-1} yr^{-1}), and 2) bog (1.4 ± 0.3 t CO2-C eq ha^{-1} yr^{-1}) peatlands. The GAM explained 99 % of the variation of total GWP for the rewetted and with RCG cultivated sites, highlighting optimal plant growth conditions as the most critical factor regarding the sites' GWP, by indicating the significant effect of biomass yield ($p < 0.001$), affecting NEE. Further, bog peatland type, soil pH, and the content of K were of minor significance (all $p < 0.05$) (Table B4).

4. Discussion

4.1. Greenhouse gas fluxes

The observed annual averages of 76 g CH_4 m^{-2} yr^{-1} for fen peatlands and 100 g CH_4 m^{-2} yr^{-1} for bogs align with reported values for wet agricultural fens (2–116 g m^{-2} yr^{-1}; Günther et al., 2015; Karki et al.,

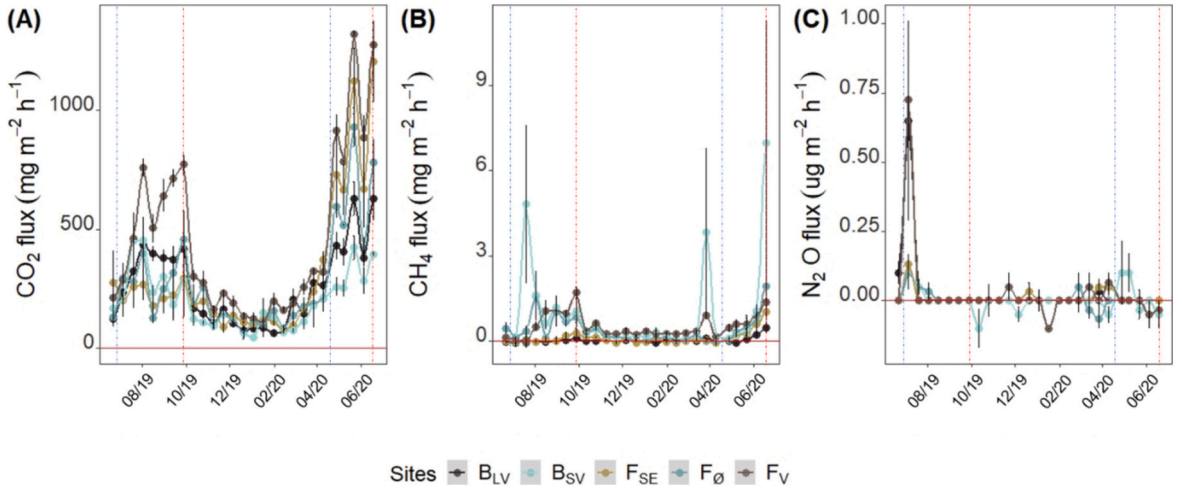


Fig. 1. Measured fluxes (in mg m^{-2} h^{-1}) for the bog (B) study sites: Lille Vildmose (B_{LV}), Store Vildmose (B_{SV}), and the fens (F): Øby ($F_Ø$), Selkær Enge (F_{SE}), and Vejrumbro (F_V). Showing A) carbon dioxide (CO_2), B) methane (CH_4) and C) nitrous oxide (N_2O). Colored lines for the various soil types show averaged flux values at the specific sampling campaigns from the replicates ($n = 4$) with standard errors showing the variation. Solid red lines indicate zero, while red dashed lines indicate harvest events on the 27th of September and 19th of June. Dashed blue lines show occurrences of fertilisation on the 24th of June and 20th of April.

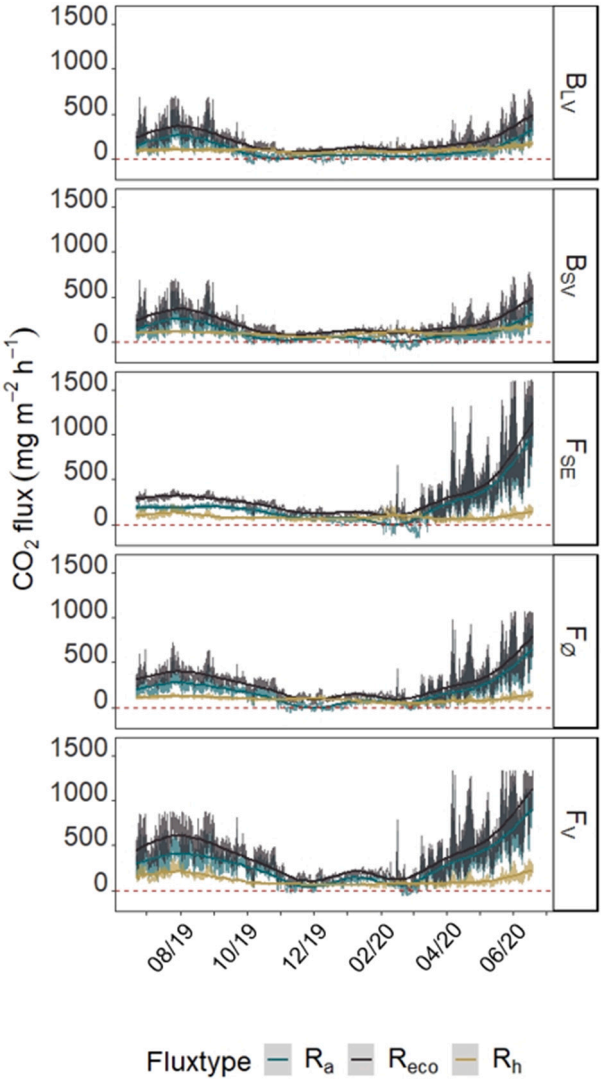


Fig. 2. Modelled hourly rates of carbon dioxide (CO_2) from autotrophic respiration (R_a), heterotrophic respiration (R_h), and the combined ecosystem respiration (R_{eco}) in g m^{-2} h^{-1} over the study period from June 2019 – June 2020 in single panels for the bog (B) study sites: Lille Vildmose (B_{LV}), Store Vildmose (B_{SV}), and the fens (F): Øby ($F_Ø$), Selkær Enge (F_{SE}), and Vejrumbro (F_V). Pale colored lines show hourly values while bold lines show smoothed averaged values over periods. Red dashed lines indicate zero.

2015; Kandel et al., 2020) and bogs (70–100 g m^{-2} yr^{-1}; Huth et al., 2020). However, a significant variability in CH_4 emissions was noted between sites, especially between bogs B_{LV} and B_{SV} (193 g CH4 m-2 yr-1 difference). The low CH4 fluxes at B_{LV} and F_{SE} may result from a WTD of −5 cm, maintaining an oxic soil layer, alongside vegetation and topsoil removal. Huth et al. (2020) found CH_4 reductions by a factor of 30–400 after topsoil removal, supported by Zak et al. (2018) and Harpenslager et al. (2015). Interestingly, RCG treatments led to 32 % to 82 % lower CH_4 emissions compared to previous studies without vegetation (Nielsen et al., 2023). This contrasts with findings that typically report higher emissions with RCG (e.g., Karki et al., 2015; Berglund et al., 2021). Grünfeld and Brix (1999) observed a 34 % reduction in CH_4 emissions with RCG cultivation, while Hyvönen et al. (2009) found lower emissions in RCG-cultivated sites. Nonetheless, The GAM explained only 56 % of the variability in CH_4 emissions, indicating complex plant-soil interactions that need further investigation (Cui et al., 2015).

Further, the negligible N_2O fluxes observed in this study, even following fertilisation, suggest that these peatland ecosystems may not contribute significantly to greenhouse gas emissions through this pathway. This can be attributed to several factors. High TC percentages in the soil likely promote denitrification processes, converting N_2O into nitrogen gas (N_2). In anaerobic conditions, denitrifying bacteria utilise N2O as an electron acceptor, effectively reducing N_2O emissions (Bastviken et al., 2011). Moreover, soil pH levels—potentially influenced by liming practices—can further suppress N_2O emissions by favoring complete denitrification reactions. Liming is known to alter microbial communities and enhance conditions that favor denitrification to N_2 (Baker et al., 2006). This is particularly relevant in peatlands, where the natural acidity can inhibit certain microbial processes. Thus,

Table 3
Average annual cumulative carbon (C) balances for soil mesocosms from Lille Vildmose (B_{LV}), Øby ($F_Ø$), Selkær Enge (F_{SE}), Store Vildmose (B_{SV}) and Vejrumbro (F_V), as well as averaged values for bog and fen peatlands. Interpolation errors resulting from the jackknife-estimates (n = 1000) for each of the carbon balances are given in brackets. Letters indicate differences between means, where treatments with the same letter are not significantly different. The global warming potential (GWP) was corrected for NEE and calculated using conversion factors of 28 for CH_4 and 265 for N_2O. Rh = Heterotrophic respiration, Ra = Autotrophic respiration, Reco = Ecosystem respiration, Biomass C = Carbon (C) export in harvested biomass, NPP = Net primary production, GPP = Gross primary production, NEE = Net ecosystem exchange, NECB = Net ecosystem carbon balance. All values in t C ha^{-1} yr^{-1} unless stated otherwise in brackets. Negative values represent uptake, positive values export to the atmosphere.

	B_{LV}	B_{SV}	$F_Ø$	F_{SE}	F_V	Bog	Fen
R_h	2.6 (± 0.1)a	2.2 (± 0.3)a	2.5 (± 0.1)a	2.1 (± 0.3)a	3.1 (± 0.2) a	2.4 (± 0.1)a	2.6 (± 0.1)a
R_a	2.7 (± 0.5) bc	2.1 (± 0.3)c	3.4 (± 0.3)bc	4.2 (± 0.8)ab	6.0 (± 0.2) a	2.4 (± 0.3)b	4.5 (± 0.4)a
R_{eco}	5.3 (± 0.5) bc	4.3 (± 0.3)c	5.9 (± 0.3)bc	6.4 (± 0.8)b	9.1 (± 0.2) a	4.8 (± 0.3)b	7.1 (± 0.5)a
Biomass C	1.2 (± 0.2) bc	0.4 (± 0.1)c	1.9 (± 0.4)ab	3.4 (± 0.6)a	2.4 (± 0.2) ab	0.8 (± 0.2)b	2.5 (± 0.3)a
NPP	3.0 (± 0.5) bc	0.9 (± 0.3)c	4.9 (± 1.0)ab	8.7 (± 1.6)a	6.2 (± 0.4) ab	1.9 (± 0.5)b	6.6 (± 0.7)a
GPP	−5.7 (± 1.0) ab	−3.0 (± 0.5)a	−8.4 (± 1.4)bc	−12.9 (± 2.1)c	−12.2 (± 0.4) c	−4.3 (± 0.7)a	−11.1 (± 1.0)b
NEE	−0.4 (± 0.5) ab	1.3 (± 0.3)a	−2.5 (± 1.0)ab	−6.5 (± 1.6)c	−3.1 (± 0.4) bc	0.4 (± 0.4)a	−4.0 (± 0.8)b
NECB	0.7 (± 0.3)a	1.7 (± 0.2)a	−0.6 (± 0.6)a	−3.2 (± 1.0)b	−0.7 (± 0.2) a	1.2 (± 0.2)a	−1.5 (± 0.5)b
CH_4 (t CO_2eq ha^{-1} yr^{-1})	0.03 (± 0.02) b	1.85 (± 0.67) a	0.76 (± 0.23) ab	0.18 (± 0.07)b	1.14 (± 0.15) ab	0.9 (± 0.5)a	0.7 (± 0.1)a
N_2O (kg CO_2eq ha^{-1} yr^{-1})	0.69 (± 0.32) a	0.04 (± 0.17) a	0.09 (± 0.1)a	0.16 (± 0.07)a	0.64 (± 0.2) a	0.4 (± 0.2)a	0.3 (± 0.1)a
GWP	0.7 (± 0.3) ab	2.2 (± 0.4)a	−0.4 (± 0.6)b	−3.1 (± 0.9)c	−0.4 (± 0.3) b	1.4 (± 0.3)a	−1.3 (± 0.5)b
GWP (t CO_2eq ha^{-1} yr^{-1})	2.7 (± 1.2) ab	7.9 (± 1.3)a	−1.3 (± 2.3)b	−11.5 (± 3.5)c	−1.4 (± 1.0) b	5.3 (± 1.3)a	−4.7 (± 1.9)b

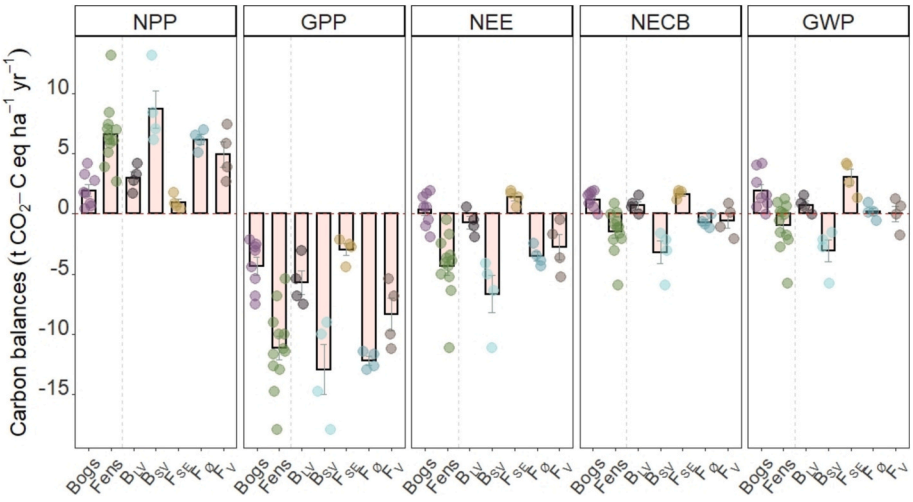


Fig. 3. Annual carbon balances of net primary production (NPP), gross primary production (GPP), net ecosystem exchange (NEE), net ecosystem carbon balance (NECB), and the global warming potential (GWP) for the study sites Lille Vildmose (B_{LV}), Øby ($F_{Ø}$), Selkær Enge (F_{SE}), Store Vildmose (B_{SV}) and Vejrumbro (F_V), as well as across the peatland types bog and fen. All values in t CO_2-C eq ha^{-1} yr^{-1}. Dots represent results per replicate, while bars indicate means across replicates, including standard error.

the combination of high TC%, favorable pH, and soil moisture levels likely contributed to the observed low N_2O fluxes, indicating that these peatland ecosystems may function as net nitrogen sinks, enhancing their overall climate mitigation potential.

4.2. Variation in GHG dynamics according to the GAM

Besides of the CH_4 and N_2O related mechanisms mentioned previously, the GAM illustrated significant variation in GHG dynamics, particularly concerning biomass growth across different peatland sites. The analysis confirmed that soil properties such as TN, BD and pH were key factors in explaining emissions of both CO_2 and CH_4. Biomass growth emerged as a key variable affecting NECB and GWP, aligning with common findings, e.g. by Roberts et al. (1993) and Nakano and Shinoda (2014), which link biomass yield to carbon dynamics.

More specific, several abiotic key points were highlighted by the GAM, affecting biomass growth and thus overall GHG dynamics:

- **Total Nitrogen (TN):** Higher TN levels correlate with increased nutrient availability, enhancing plant growth and biomass productivity. This is particularly relevant in wetland ecosystems, where nitrogen often limits vegetation. In our study, fen peatlands exhibited higher TN levels compared to bogs, possibly explaining the greater biomass yields observed in fen sites. Elevated TN can foster a more vigorous microbial community, facilitating organic matter decomposition and enhancing carbon cycling. The higher N availability on our fen soils however is not only a relic from previous agricultural use (i.e. fertilisation, Liu et al., 2023), but also a semi-naturally occurring phenomenon due to winter flooding and the related N loads in water (Elberling et al., 2023).
- **Bulk Density (BD):** BD is a critical indicator of soil compaction and porosity, directly affecting root penetration and water movement (Strock et al., 2022). Lower BD values typically indicate better soil structure, allowing for optimal root growth and improved water retention. The differences in BD between fen and bog peatlands likely influenced both biomass productivity and GHG emissions, with fens generally promoting better aeration and moisture retention.
- **pH Levels:** Soil pH significantly impacts nutrient availability and microbial activity. In our study, higher pH levels in fen peatlands positively correlated with biomass production while negatively impacting N_2O emissions. Higher pH enhances microbial processes that favor complete denitrification, effectively reducing N_2O emissions (Baker et al., 2006). Conversely, lower pH in bogs may inhibit denitrification pathways, contributing to higher N_2O emissions under certain conditions. This dual role of pH underscores its importance in peatland management. The legacy effect of liming on pH levels in previously agriculturally used peatlands, and those used in this study, is a crucial consideration for future land management such as paludiculture. While liming raises soil pH and improves nutrient availability—benefiting crops like reed canary grass (RCG)—its effects can persist over multiple growing seasons. This legacy can foster a favorable environment for plant growth, enhancing biomass productivity and potentially increasing carbon sequestration (Hamilton et al., 2007). However, continuous liming in the past may also have disrupted the natural balance of nutrients and microbial communities that thrive in acidic conditions (Grover et al., 2021; Biasi et al., 2008). Excessive alkalinisation can limit the availability of essential micronutrients, such as iron and manganese, affecting plant health – and at the end biomass growth and thus: GHG dynamics.
- **Biomass Growth and Yield:** The consistent biomass growth observed across sites until the first cut in September 2019 indicated a favorable initial response of both fen and bog peatlands to management practices. However, the significant difference in cumulative biomass yield—averaging 5.6 t DM ha^{-1} yr^{-1} for fen peatlands compared to 1.7 t DM ha^{-1} yr^{-1} for bogs—highlights inherent productivity disparities. The highest yield recorded for F_{SE} (7.4 t DM ha^{-1} yr^{-1}) and the notably low yield for B_{SV} (0.8 t DM ha^{-1} yr^{-1}) emphasise the potential for enhanced biomass production in fen systems. Strong positive correlations between biomass yields and soil contents of sulfur (S), iron (Fe), BD, and TN suggested that these properties are crucial for biomass productivity. Conversely, the negative correlation between TC and the C/N ratio indicates that higher nitrogen availability may facilitate biomass growth by enhancing nutrient uptake. The positive correlation of pH with S, P, and Fe underscores the importance of soil chemistry in influencing plant productivity and carbon dynamics.
- **GHG fluxes and C balances:** Measured fluxes of CO_2, CH_4, and N_2O showed distinct patterns influenced by biomass growth and environmental factors. CO_2 fluxes were significantly higher in sites with

robust biomass growth, aligning with studies linking productivity to carbon respiration processes. Lower CH_4 fluxes, particularly in mesocosms with a WTD of −5 cm, suggest that anaerobic conditions, which typically enhance methane production, were not consistently met. The occurrence of methane uptake in specific sites, especially B_{LV}, indicated a complex interplay of aerobic and anaerobic processes, warranting further investigation into microbial dynamics. The GAM effectively captured a significant portion of the variability in CO_2 and CH_4 fluxes, demonstrating the critical role of biomass growth and temperature interactions. The model explained 85 % of the deviance in CO_2 and 56 % for CH_4 emissions, indicating that while biomass is a key driver, other factors—including soil temperature and moisture dynamics—also play vital roles. The annual cumulative emissions and carbon balances further illustrated the contrasting roles of fen and bog peatlands in carbon cycling. The negative NEE observed in sites with high biomass growth suggests these ecosystems may act as significant carbon sinks, particularly in fen systems. Conversely, the positive NEE in less productive bog sites indicates a net carbon release, underscoring the importance of site management and vegetation cover in influencing carbon dynamics.

4.3. GHG budgets

The GHG budgets calculated for the study sites showed significant differences between fen and bog peatlands. Fens exhibited a negative GWP, averaging −4.7 t CO_2eq ha^{-1} yr^{-1}, indicating their role as carbon sinks, while bogs displayed positive GWPs, averaging 5.3 t CO_2eq ha^{-1} yr^{-1}, suggesting they functioned as net carbon sources. These findings aligned with previous research on GHG emissions from rewetted temperate fens (Günther et al., 2015; Hemes et al., 2019; Kandel et al., 2020) and bogs (Beyer and Höper, 2015; Swenson et al., 2019), highlighting the importance of site-specific factors in GHG dynamics. The calculated GWPs illustrated the nuanced carbon balance of these peatland types, with fen peatlands showing a GWP of −1.3 t CO_2-C eq ha^{-1} yr^{-1} and bog peatlands a positive GWP of 1.4 t CO_2-C eq ha^{-1} yr^{-1}.

With negligible N_2O emissions and minimal CH_4 contributions, it became clear that the carbon sink or source potential was primarily determined by CO_2 balances. The GAM indicated that biomass development was a critical component of carbon balances (Roberts et al., 1993; Skinner, 2008; Nakano and Shinoda, 2014), scaling with net primary production (NPP) (Enquist et al., 2017). Comparisons of net GHG budgets for paludiculture studies could have led to biased conclusions if biomass yields were not comparable. For example, the NECB for mesocosms from Øby ($F_Ø$) was -0.6 ± 0.6 t C ha^{-1} yr^{-1}, while a field trial at the same site found an NECB of 0.7 t C ha^{-1} yr^{-1} (Kandel et al., 2020). Significant variability in NPP was observed during the first year of establishment, indicating that RCG might have been unsuitable for rewetted bogs, where yields could drop to 1.0 t DM ha^{-1} yr^{-1} (Kukk et al., 2011). In contrast, first-year yields from fen mesocosms were similar to those reported in established field trials (Kandel et al., 2013; Karki et al., 2019; Nielsen et al., 2021a). Overall, NPP outpaced Rh across most sites, and the pronounced effect of biomass was evident in GPP differences. The net GHG balances were consistent with previous reports, showing substantial site-specific variations (Beyer and Höper, 2015; Swenson et al., 2019).

While rewetting and RCG cultivation increased CH_4 emissions compared to the drained state (Nielsen et al., 2023), three of five sites were either climate neutral or acted as carbon sinks. Interannual variability was expected; for instance, Karki et al. (2019) and Kandel et al. (2019) documented significant differences in GHG balances at Ø, with a variation of 11.1 t CO2eq ha^{-1} yr^{-1} between years. Our mesocosm experiment indicated a stronger C sink for the same site, attributed to stable WTD control and resulting lower CH_4 emissions compared to earlier studies (Kandel et al., 2020), likely influenced by partial topsoil removal (Harpenslager et al., 2015; Huth et al., 2020). In comparison, RCG cultivation on drained peat soils had shown GWPs between 3.6 (Järveoja et al., 2016) and 9.1 t CO_2eq ha^{-1} yr^{-1} (Kasimir et al., 2017). Our results suggested that rewetting and RCG cultivation on fen peatlands could mitigate GHG emissions by up to 11 t CO_2eq ha^{-1} yr^{-1}, consistent with previously reported emission reductions (Günther et al., 2015; Wilson et al., 2016; de Jong et al., 2021).

5. Conclusion

This study highlighted distinct site-specific variations in biomass yields attributed to soil geochemical properties, which either facilitate or hinder biomass growth, subsequently affecting ecosystem respiration. Overall emissions from the studied sites were dominated by CO_2 in relation to NPP. The controlled mesocosm experiment enabled a meaningful comparison of geographically isolated peatlands regarding their GHG budgets, highlighting significant variations in GWPs that reflected site-specific differences impacting biogeochemical processes and biomass growth. In this study, the three fen peatlands emerged as net carbon sinks during the first year following rewetting and RCG establishment, while indicating the potential unsuitability of rewetted bog peatlands for RCG cultivation. Fen peatlands exhibited the highest combined efficiencies for biomass production and emission reduction, emphasising that GHG mitigation potential is closely linked to soil-specific biogeochemistry, with pH and soil fertility as key variables. The correlation between higher TN levels and increased biomass productivity underscored the critical role of nutrient availability, while the legacy effects of liming practices on reducing N_2O emissions provide future management implications. By focusing on RCG cultivation in rewetted peatlands, this research fills a gap in the literature regarding GHG dynamics during the establishment year of paludiculture, thus enhancing understanding of its potential as a sustainable land-use option for climate change mitigation. The comparative analysis of five distinct peatland types not only highlighted the necessity for evidence-based recommendations for effective land management but also supports national and international goals of rewetting agricultural soils. Ultimately, these findings contribute to the development of sustainable agricultural practices that align productivity with climate mitigation goals, while advocating for multi-annual measurements to assess long-term trends in GHG balances and the role of soil microbial dynamics in these processes.

CRediT authorship contribution statement

C.K. Nielsen: Writing – review & editing, Writing – original draft, Visualization, Methodology, Investigation, Formal analysis, Data curation, Conceptualization. **L. Elsgaard:** Writing – review & editing. **P.E. Lærke:** Writing – review & editing, Supervision, Funding acquisition.

Funding

This study was financially supported by the PEATWISE project (https://www.eragas.eu/en/eragas/Research-projects/PEATWISE.htm) in the frame of the ERA-NET FACCE ERA-GAS. FACCE ERA-GAS received funding from the European Union's Horizon 2020 research and innovation program under the grant agreement no. 696356. This publication further was funded by the Interreg project CANAPE under the North Sea Region Programme and the European Regional Development Fund. In addition, the study was partly supported by the Aarhus University Centre for Circular Bioeconomy (CBIO, https://cbio.au.dk/en/). Further, CN received funding by the European Union's Horizon Europe programme (WET HORIZONS, grant agreement no. 101056848).

Declaration of competing interest

The authors declare that the research was conducted in the absence of any commercial or financial relationships that could be construed as a potential conflict of interest.

Acknowledgements

The authors want to thank the technical and laboratory staff at the Department of Agroecology, and in particular Michael Koppelgaard and Bodil Stensgaard, for excellent support during stages of study set-up as well as laboratory analyses.

Appendix A. Supplementary data

Supplementary data to this article can be found online at https://doi.org/10.1016/j.scitotenv.2024.177677.

Data availability

The raw data supporting the conclusions of this article will be made available by the authors, without undue reservation.

References

Asemaninejad, A., Thorn, R.G., Branfireun, B.A., Lindo, Z., 2019. Vertical Stratification of Peatland Microbial Communities Follows a Gradient of Functional Types across Hummock–Hollow Microtopographies. Ecoscience 26 (3), 249-258, 210. doi:1080/11956860.2019.1595932.

Baker, D.F., et al., 2006. TransCom 3 inversion intercomparison: Impact of transport model errors on the interannual variability of regional CO_2 fluxes, 1988–2003. Global Biogeochem. Cycles 20, GB1002. https://doi.org/10.1029/2004GB002439.

Bastviken, D., Tranvik, L.J., Downing, J.A., Crill, P.M., Enrich-Prast, A., 2011. Freshwater methane emissions offset the continental carbon sink. Science 331 (6013), 50. https://doi.org/10.1126/science.1196808. PMID: 21212349.

Beetz, S., Liebersbach, H., Glatzel, S., Jurasinski, G., Buczko, U., Höper, H., 2013. Effects of land use intensity on the full greenhouse gas balance in an Atlantic peat bog. Biogeosciences 10 (2), 1067–1082. https://doi.org/10.5194/bg-10-1067-2013.

Berglund, Ö., Kätterer, T., Meurer, K.H.E., 2021. Emissions of CO2, N2O and CH4 from cultivated and set aside drained peatland in Central Sweden. Front. Environ. Sci. 9 (25). https://doi.org/10.3389/fenvs.2021.630721.

Beyer, C., Höper, H., 2015. Greenhouse gas exchange of rewetted bog peat extraction sites and a Sphagnum cultivation site in Northwest Germany. Biogeosciences 12 (7), 2101–2117. https://doi.org/10.5194/bg-12-2101-2015.

Biasi, C., Lind, S.E., Pekkarinen, N.M., Huttunen, J.T., Shurpali, N.J., Hyvönen, N.P., Martikainen, P.J., 2008. Direct experimental evidence for the contribution of lime to CO2 release from managed peat soil. Soil Biol. Biochem. 40 (10), 2660–2669. https://doi.org/10.1016/j.soilbio.2008.07.011.

Chapman, S., Buttler, A., Francez, A.-J., Laggoun-Défarge, F., Vasander, H., Schloter, M., . . . Mitchell, E., P. (2003). Exploitation of northern peatlands and biodiversity maintenance: a conflict between economy and ecology. Front. Ecol. Environ., 1(10), 525–532. Retrieved from https://hal-insu.archives-ouvertes.fr/hal-00069337.

Conchedda, G., Tubiello, F.N., 2020. Drainage of organic soils and GHG emissions: validation with country data. Earth Syst. Sci. Data 12 (4), 3113–3137. https://doi.org/10.5194/essd-12-3113-2020.

Cui, M., Ma, A., Qi, H., Zhuang, X., Zhuang, G., 2015. Anaerobic oxidation of methane: an "active" microbial process, 4(1), pp. 1–11. https://doi.org/10.1002/mbo3.232.

Eickenscheidt, T., Heinichen, J., Drösler, M., 2015. The greenhouse gas balance of a drained fen peatland is mainly controlled by land-use rather than soil organic carbon content. Biogeosciences 12 (17), 5161–5184. https://doi.org/10.5194/bg-12-5161-2015.

Elberling, B.B., Kovács, G.M., Hansen, H.F.E., et al., 2023. High nitrous oxide emissions from temporary flooded depressions within croplands. Commun. Earth Environ. 4, 463. https://doi.org/10.1038/s43247-023-01095-8.

Elsgaard, L., Görres, C.-M., Hoffmann, C.C., Blicher-Mathiesen, G., Schelde, K., Petersen, S.O., 2012. Net ecosystem exchange of CO2 and carbon balance for eight temperate organic soils under agricultural management. Agr Ecosyst Environ 162, 52–67. https://doi.org/10.1016/j.agee.2012.09.001.

Enquist, B.J., Bentley, L.P., Shenkin, A., Maitner, B., Savage, V., Michaletz, S., Blonder, B., Buzzard, V., Espinoza, T.E.B., Farfan-Rios, W., et al., 2017. Assessing trait-based scaling theory in tropical forests spanning a broad temperature gradient. Glob. Ecol. Biogeogr. 26, 1357–1373. https://doi.org/10.1111/geb.12645.

Evans, C.D., Peacock, M., Baird, A.J., Artz, R.R.E., Burden, A., Callaghan, N., Morrison, R., 2021. Overriding water table control on managed peatland greenhouse gas emissions. Nature 593 (7860), 548–552. https://doi.org/10.1038/s41586-021-03523-1.

Grover, S.P., Butterly, C.R., Wang, X., Gleeson, D.B., Macdonald, L.M., Tang, C., 2021. Liming and priming: the long-term impact of pH amelioration on mineralisation may negate carbon sequestration gains. Soil Security 3, 100007. https://doi.org/10.1016/j.soisec.2021.100007.

Grünfeld, S., Brix, H., 1999. Methanogenesis and methane emissions: effects of water table, substrate type and presence of Phragmites australis. Aquatic Botany 64 (1), 63–75. https://doi.org/10.1016/S0304-3770(99)00010-8.

Günther, A., Huth, V., Jurasinski, G., Glatzel, S., 2015. The effect of biomass harvesting on greenhouse gas emissions from a rewetted temperate fen. GCB Bioenergy 7 (5), 1092–1106. https://doi.org/10.1111/gcbb.12214.

Hamilton, S.K., Kurzman, A.L., Arango, C., Jin, L., Robertson, G.P., 2007. Evidence for carbon sequestration by agricultural liming. Global Biogeochem. Cycles 21, GB2021. https://doi.org/10.1029/2006GB002738.

Harpenslager, S.F., van den Elzen, E., Kox, M.A., Smolders, A.J., Ettwig, K.F., Lamers, L. P., 2015. Rewetting former agricultural peatlands: topsoil removal as a prerequisite to avoid strong nutrient and greenhouse gas emissions. Ecol. Eng. 84, 159–168. https://doi.org/10.1016/j.ecoleng.2015.08.002.

Hartung, C., Andrade, D., Dandikas, V., Eickenscheidt, T., Drösler, M., Zollfrank, C., Heuwinkel, H., 2020. Suitability of paludiculture biomass as biogas substrate – biogas yield and long-term effects on anaerobic digestion. Renew. Energy 159, 64–71 doi:1016/j.renene.2020.05.156.

Hemes, K.S., Chamberlain, S.D., Eichelmann, E., Anthony, T., Valach, A., Kasak, K., Baldocchi, D.D., 2019. Assessing the carbon and climate benefit of restoring degraded agricultural peat soils to managed wetlands. Agric. For. Meteorol. 268, 202–214. https://doi.org/10.1016/j.agrformet.2019.01.017.

Huth, V., Günther, A., Jurasinski, G., Glatzel, S.J.M., Peat., 2013. The effect of an exceptionally wet summer on methane effluxes from a 15-year re-wetted fen in north-east Germany, 13(02), pp. 1–7.

Huth, V., Hoffmann, M., Bereswill, S., Popova, Y., Zak, D., Augustin, J., 2018. The climate warming effect of a fen peat meadow with fluctuating water table is reduced by young alder trees. Mires & Peat 21. https://doi.org/10.19189/MaP.2017.OMB.291.

Huth, V., Günther, A., Bartel, A., Hofer, B., Jacobs, O., Jantz, N., Jurasinski, G., 2020. Topsoil removal reduced in-situ methane emissions in a temperate rewetted bog grassland by a hundredfold. Sci. Total Environ. 721. https://doi.org/10.1016/j.scitotenv.2020.137763.

Hyvönen, N.P., Huttunen, J.T., Shurpali, N.J., Tavi, N.M., Repo, M.E., Martikainen, P.J., 2009. Fluxes of nitrous oxide and methane on an abandoned peat extraction site: effect of reed canary grass cultivation. Bioresour. Technol. 100 (20), 4723–4730. https://doi.org/10.1016/j.biortech.2009.04.043.

Järveoja, J., Peichl, M., Maddison, M., Teemusk, A., Mander, Ü., 2016. Full carbon and greenhouse gas balances of fertilized and nonfertilized reed canary grass cultivations on an abandoned peat extraction area in a dry year. GCB Bioenergy 8 (5), 952–968. https://doi.org/10.1111/gcbb.12308.

Jensen, A.B., Eller, F., 2020. Hybrid Napier grass (Pennisetum purpureum Schumach × P. Americanum (L.) Leeke cv. Pakchong1) and Giant reed (Arundo donax L.) as candidate species in temperate European paludiculture: growth and gas exchange responses to suboptimal temperatures. Aquat. Bot. 160, 103165. https://doi.org/10.1016/j.aquabot.2019.103165.

de Jong, M., van Hal, O., Pijlman, J., van Eekeren, N., Junginger, M., 2021. Paludiculture as paludifuture on Dutch peatlands: an environmental and economic analysis of Typha cultivation and insulation production. Sci. Total Environ. 792, 148161. https://doi.org/10.1016/j.scitotenv.2021.148161.

Jurasinski, G., Koebsch, F., Guenther, A., Beetz, S., 2014. Flux: flux rate calculation from dynamic closed chamber measurements. R package version 0.3-0. https://CRAN.R-project.org/package=flux.

Juszczak, R., Humphreys, E., Acosta, M., Michalak-Galczewska, M., Kayzer, D., Olejnik, J., 2013. Ecosystem respiration in a heterogeneous temperate peatland and its sensitivity to peat temperature and water table depth. Plant and Soil 366 (1), 505–520. https://doi.org/10.1007/s11104-012-1441-y.

Juutinen, A., Tolvanen, A., Saarimaa, M., Ojanen, P., Sarkkola, S., Ahtikoski, A., Tuominen, S., 2020. Cost-effective land-use options of drained peatlands– integrated biophysical-economic modeling approach. Ecol. Econ. 175, 106704. https://doi.org/10.1016/j.ecolecon.2020.106704.

Kalhori, A., Wille, C., Gottschalk, P., et al., 2024. Temporally dynamic carbon dioxide and methane emission factors for rewetted peatlands. Commun Earth Environ 5, 62. https://doi.org/10.1038/s43247-024-01226-9.

Kandel, T.P., Elsgaard, L., Laerke, P.E., 2013. Measurement and modelling of CO2flux from a drained fen peatland cultivated with reed canary grass and spring barley. GCB Bioenergy 5 (5), 548–561. https://doi.org/10.1111/gcbb.12020.

Kandel, T.P., Karki, S., Elsgaard, L., Lærke, P.E., 2019. Fertilizer-induced fluxes dominate annual N<inf>2</inf>O emissions from a nitrogen-rich temperate fen rewetted for paludiculture. Nutr. Cycl. Agroecosyst. 115 (1), 57–67. https://doi.org/10.1007/s10705-019-10012-5.

Kandel, T.P., Karki, S., Elsgaard, L., Labouriau, R., Lærke, P.E., 2020. Methane fluxes from a rewetted agricultural fen during two initial years of paludiculture. Sci. Total Environ. 713. https://doi.org/10.1016/j.scitotenv.2020.136670.

Karki, S., Elsgaard, L., Audet, J., Lærke, P.E., 2014. Mitigation of greenhouse gas emissions from reed canary grass in paludiculture: effect of groundwater level. Plant and Soil 383 (1), 217–230. https://doi.org/10.1007/s11104-014-2164-z.

Karki, S., Elsgaard, L., Lærke, P.E., 2015. Effect of reed canary grass cultivation on greenhouse gas emission from peat soil at controlled rewetting. Biogeosciences 12 (2), 595–606. https://doi.org/10.5194/bg-12-595-2015.

Karki, S., Elsgaard, L., Kandel, T.P., Lærke, P.E., 2016. Carbon balance of rewetted and drained peat soils used for biomass production: a mesocosm study. GCB Bioenergy 8 (5), 969–980. https://doi.org/10.1111/gcbb.12334.

Karki, S., Kandel, T., Elsgaard, L., Labouriau, R., Lærke, P., 2019. Annual CO 2 fluxes from a cultivated fen with perennial grasses during two initial years of rewetting. Mires & Peat 25. https://doi.org/10.19189/MaP.2017.DW.322.

Kasimir, Å., He, H., Coria, J., Nordén, A., 2017. Land use of drained peatlands: greenhouse gas fluxes, plant production, and economics. Glob. Chang. Biol. 24 (8), 3302–3316. https://doi.org/10.1111/gcb.13931.

Köhler, W., Schachtel, G., Voleske, P., 2012. Biostatistik: Eine Einführung für Biologen und Agrarwissenschaftler. Springer-Verlag.

Kukk, L., Roostalu, H., Suuster, E., Rossner, H., Shanskiy, M., Astover, A., 2011. Reed canary grass biomass yield and energy use efficiency in northern European

pedoclimatic conditions. Biomass Bioenergy 35 (10), 4407–4416. https://doi.org/10.1016/j.biombioe.2011.08.018.
Lahtinen, L., Mattila, T., Myllyviita, T., Seppälä, J., Vasander, H., 2022. Effects of paludiculture products on reducing greenhouse gas emissions from agricultural peatlands. Ecol. Eng. 175, 106502. https://doi.org/10.1016/j.ecoleng.2021.106502.
Liobikienė, G., Butkus, M., 2017. The European Union possibilities to achieve targets of Europe 2020 and Paris agreement climate policy. Renew. Energy 106 (C), 298–309. Retrieved from. https://EconPapers.repec.org/RePEc:eee:renene:v:106:y:2017:i:c:p:298-309.
Liu, W., Fritz, C., van Belle, J., Nonhebel, S., 2023. Production in peatlands: comparing ecosystem services of different land use options following conventional farming. Sci. Total Environ. 875, 162534. https://doi.org/10.1016/j.scitotenv.2023.162534.
Lloyd, J., Taylor, J.A., 1994. On the temperature dependence of soil respiration. Functional Ecology 8 (3), 315–323. https://doi.org/10.2307/2389824.
Marra, G., Wood, S.N., 2011. Practical variable selection for generalized additive models. Computational Statistics & Data Analysis 55 (7), 2372–2387. https://doi.org/10.1016/j.csda.2011.02.004.
McCarthy, M.C., Enquist, B.J., 2007. Consistency between an Allometric approach and optimal partitioning theory in global patterns of plant biomass allocation. Funct. Ecol. 21 (4), 713–720. Retrieved from. http://www.jstor.org/stable/4540076.
Ministry of Food, Agriculture and Fisheries of Denmark, 2021. Overblik over arealkategorier vedr. udtagning af kulstofrige landbrugsjorder. MOF Alm. del Bilag 514. Available at: https://www.ft.dk/samling/20201/almdel/MOF/bilag/514/2382777.pdf (accessed 0707, 2021).
Montanarella, Luca, Jones, R.J.A., Hiederer, R., 2006. The distribution of peatland in Europe. Mires and Peat 1, 01. http://www.mires-and-peat.net. ISSN 1819-754X.
Myhre, G., Shindell, D., Bréon, F.-M., Collins, W., Fuglestvedt, J., Huang, J., Koch, D., Lamarque, J.-F., Lee, D., Mendoza, B., Nakajima, T., Robock, A., Stephens, G., Takemura, T., Zhang, H., 2013. Anthropogenic and Natural Radiative Forcing. In: Stocker, T.F., Qin, D., Plattner, G.-K., Tignor, M., Allen, S.K., Boschung, J., Nauels, A., Xia, Y., Bex, V., Midgley, P.M. (Eds.), Climate Change 2013: The Physical Science Basis. Contribution of Working Group I to the Fifth Assessment Report of the Intergovernmental Panel on Climate Change. Cambridge University Press, Cambridge, United Kingdom and New York, NY, USA.
Nakano, T., Shinoda, M., 2014. Spatial variability of photosynthetic production and ecosystem respiration on a hundred-kilometer scale within a Mongolian semiarid grassland. Journal of Agricultural Meteorology 70 (2), 105–116. https://doi.org/10.2480/agrmet.d-13-00026.
Nielsen, C.K., Stødkilde, L., Jørgensen, U., Lærke, P.E., 2021a. Effects of harvest and fertilization frequency on protein yield and extractability from flood-tolerant perennial grasses cultivated on a fen peatland. Front. Environ. Sci. 9. https://doi.org/10.3389/fenvs.2021.619258.
Nielsen, C.K., Jørgensen, U., Lærke, P.E., 2021b. Root-to-shoot ratios of flood-tolerant perennial grasses depend on harvest and fertilization management: implications for quantification of soil carbon input. Front. Environ. Sci. 9. https://doi.org/10.3389/fenvs.2021.785531.
Nielsen, C.K., Elsgaard, L., Jørgensen, U., Lærke, P.E., 2023. Soil greenhouse gas emissions from drained and rewetted agricultural bare peat mesocosms are linked to geochemistry. Sci. Total Environ. 896, 165083. https://doi.org/10.1016/j.scitotenv.2023.165083.
Oertel, C., Matschullat, J., Zurba, K., Zimmermann, F., Erasmi, S., 2016. Greenhouse gas emissions from soils—a review. Geochemistry 76 (3), 327–352. https://doi.org/10.1016/j.chemer.2016.04.002.
Petersen, S.O., Hoffmann, C.C., Schäfer, C.M., Blicher-Mathiesen, G., Elsgaard, L., Kristensen, K., Greve, M.H., 2012. Annual emissions of CH4 and N2O, and ecosystem respiration, from eight organic soils in Western Denmark managed by agriculture. Biogeosciences 9 (1), 403–422. https://doi.org/10.5194/bg-9-403-2012.
R Core Team, 2021. R: A Language and Environment for Statistical Computing. R Foundation for Statistical Computing, Vienna, Austria. URL: https://www.R-project.org/.
Roberts, M.J., Long, S.P., Tieszen, L.L., Beadle, C.L., 1993. Measurement of plant biomass and net primary production of herbaceous vegetation. In: Hall, D.O., Scurlock, J.M.O., Bolhàr-Nordenkampf, H.R., Leegood, R.C., Long, S.P. (Eds.), Photosynthesis and Production in a Changing Environment: A Field and Laboratory Manual. Springer Netherlands, Dordrecht, pp. 1–21.
Skinner, R.H., 2008. High biomass removal limits carbon sequestration potential of mature temperate pastures. J. Environ. Qual. 37 (4), 1319–1326. https://doi.org/10.2134/jeq2007.0263.
Smith, K.A., Ball, T., Conen, F., Dobbie, K.E., Massheder, J., Rey, A., 2018. Exchange of greenhouse gases between soil and atmosphere: interactions of soil physical factors and biological processes. Eur. J. Soil Sci. 69 (1), 10–20. https://doi.org/10.1111/ejss.12539.
Solomon, S., Plattner, G.-K., Knutti, R., Friedlingstein, P., 2009. Irreversible climate change due to carbon dioxide emissions. Proc. Natl. Acad. Sci. 106 (6), 1704–1709. https://doi.org/10.1073/pnas.0812721106.
Stewart, R.I.A., Dossena, M., Bohan, D.A., Jeppesen, E., Kordas, R.L., Ledger, M.E., Woodward, G., 2013. Chapter two - mesocosm experiments as a tool for ecological climate-change research. In: Woodward, G., O'Gorman, E.J. (Eds.), Advances in Ecological Research, vol. 48. Academic Press, pp. 71–181.
Strock, C.F., Rangarajan, H., Black, C.K., Schäfer, E.D., Lynch, J.P., 2022. Theoretical evidence that root penetration ability interacts with soil compaction regimes to affect nitrate capture. Ann. Bot. 129 (3), 315–330. https://doi.org/10.1093/aob/mcab144.
Swenson, M.M., Regan, S., Bremmers, D.T.H., Lawless, J., Saunders, M., Gill, L.W., 2019. Carbon balance of a restored and cutover raised bog: implications for restoration and comparison to global trends. Biogeosciences 16 (3), 713–731. https://doi.org/10.5194/bg-16-713-2019.
Tanneberger, F., Schröder, C., Hohlbein, M., Lenschow, U., Permien, T., Wichmann, S., Wichtmann, W., 2020. Climate change mitigation through land use on rewetted peatlands – cross-sectoral spatial planning for Paludiculture in Northeast Germany. Wetlands 40 (6), 2309–2320. https://doi.org/10.1007/s13157-020-01310-8.
Wilson, D., Blain, D., Couwenberg, J., Evans, C., Murdiyarso, D., Page, S., Strack, M., 2016. Greenhouse gas emission factors associated with rewetting of organic soils. Mires and Peat 17.
Wood, S.N., 2011. Fast stable restricted maximum likelihood and marginal likelihood estimation of semiparametric generalized linear models. J. R. Stat. Soc. Series B Stat. Methodology 73 (1), 3–36 doi:1111/j.1467-9868.2010.00749.x.
Wood, S.N., Pya, N., Säfken, B., 2016. Smoothing parameter and model selection for general smooth models. J. Am. Stat. Assoc. 111 (516), 1548–1563. https://doi.org/10.1080/01621459.2016.1180986.
Zak, D., Goldhammer, T., Cabezas, A., Gelbrecht, J., Gurke, R., Wagner, C., McInnes, R., 2018. Top soil removal reduces water pollution from phosphorus and dissolved organic matter and lowers methane emissions from rewetted peatlands. J. Appl. Ecol. 55 (1), 311–320. https://doi.org/10.1111/1365-2664.12931.
Ziegler, R., Wichtmann, W., Abel, S., Kemp, R., Simard, M., Joosten, H., 2021. Wet peatland utilisation for climate protection – an international survey of paludiculture innovation. Cleaner Engineering and Technology 5, 100305 doi:1016/j.clet.2021.100305.